Memoirs of the Faculty of Engineering and Design
Kyoto Institute of Technology 54 (March, 2006)

Observer-based Collision Detection and Its Spot Estimation of a Flexible Cantilevered Beam Using Ratio of Mode Functions

Yuichi SAWADA

Abstract

This paper presents a method of collision detection and its spot estimation on flexible cantilevered beam. The relevant beam is modeled by an Euler-Bernoulli type partial differential equation with an external (unknown) force due to a collision and a Kelvin-Voigt type internal damping term. The collision event is assumed to be caused by an unexpected obstacle that collides with a spot of the beam, which is mathematically characterized by the Dirac's delta function with an unknown position and magnitude. The estimates of the beam's state and the collision input in modal representation are obtained, using an observer which decouples the effect of the collision input to an estimation error. Introducing a scalar function which is defined by the ratio of the modal collision inputs corresponding to the first two modes, the collision spot can be estimated using the inverse of the ratio of mode functions. The efficacy of the proposed method is demonstrated by some numerical simulations

Key Words: *flexible cantilevered beam; observer; collision detection; collision spot; mode functions*

1. Introduction

In the near future, robotic manipulators will be used in a highly structured environment such as living space in houses, hospitals, offices and so on. One of the specifications of the manipulators used in such environments is to prevent collision with (mobile) objects in the manipulator's workspace. From the viewpoint of safety, the use of flexible manipulators gives us an advantage, because such manipulators are light weighted and mechanically flexible. However, the collision with an unexpected obstacle or other operated objects is a serious problem for the flexible manipulator and the obstacle. In order to avoid damage to them, caused by the collision, collision detection and the estimation of the spot where the obstacle collides will play a significant role for the flexible manipulators in operation. As for multi-link flexible manipulators, obtaining the information of the collision spot on the arm is important for replanning the path of the manipulator in order to avoid the obstacle.

Contact/collision between a flexible manipulator and environmental objects has been investigated by some researchers. Matsuno, *et al.*[1] studied the modeling and control of flexible manipulators contacting with environmental objects based on the strain feedback control. Ching and Wang[2] presented a stability analysis of a single-link flexible manipulator in collision. The collision detection mechanisms for flexible manipulators/structures have been studied.[3)-7)] Kaneko, *et al.*[3),4)] developed an active antenna for mobile

robots. They used the deformation of a flexible beam for measuring a position of contact with an object. Moorehead and Wang[5] proposed a collision detection method using strain gauges to determine the intensity and the position of externally applied force due to collision acting on a flexible cantilevered beam. The position estimation of the contact in their approach was given by the mechanical relation between the positions of two strain gauges and the bending moments at the sensors' locations. The author[6)-8)] proposed a collision detection algorithm for a flexible cantilevered beam subject to distributed random disturbance based on an innovation process. He also investigated an estimation method of the collision force acting on a flexible beam[9),10)] and a method of collision spot estimation using the Kalman filter for an augmented system composed by a second-order model for the collision input and a system model of the flexible beam.[11)]

This paper presents a method of collision detection and its spot estimation of a flexible cantilevered beam based on an observer which decouples the effect of collision from an estimation error. The mathematical model of the beam is described by an Euler-Bernoulli type partial differential equation with a collision term (collision input). The obstacle is assumed to collide with a point on the beam. The approach to the estimation of the collision spot is to calculate the inverse of a scalar function which is defined by a ratio of the modal representation collision inputs corresponding to the first two modes. In order to demonstrate the performance of the proposed method, several numerical results are provided.

2. Mathematical Model of Flexible Beam

Consider a uniform Euler-Bernoulli type cantilevered beam with unknown input caused by a collision with an unexpected obstacle. The mathematical model of the beam is described by the following partial differential equation:

$$\rho S\frac{\partial^2 u(t,x)}{\partial t^2} + c_D I\frac{\partial^5 u(t,x)}{\partial x^4 \partial t} + EI\frac{\partial^4 u(t,x)}{\partial x^4} = g\, s(t)\, \delta(x - x_c), \qquad (0 < x < \ell) \tag{1}$$

where $u(t,x)$ denotes the transverse displacement from its equilibrium state of the beam at the time t and the position x; ρ the mass density; S the cross sectional area of the beam; E the Young's modulus; I the second moment of cross sectional area; c_D the coefficient of the Kelvin-Voigt type damping; g a constant. The collision is assumed to be made with a single spot of the beam, *i.e.*, $x = x_c$ which is an unknown parameter. $s(t)$ denotes the external force (collision input) caused by the collision with an unexpected obstacle. $s(t)$ takes nonzero value while the obstacle collides with the beam. It can be expressed by

$$s(t) = \begin{cases} 0, & t < t_c \\ s_0(t), & t_c \le t \le t_e \\ 0, & t_e < t, \end{cases} \tag{2}$$

where $s_0(t)$ denotes the unknown function which gives the behavior of the collision force's strength in the time interval $t \in [t_c,\ t_e]$ (t_c, t_e: unknown parameters). The boundary and initial conditions of eq.(1) are given by

$$\text{I.C.: } u(0,x) = u_0(x), \quad \dot{u}(0,x) = \dot{u}_0(x) \tag{3}$$

$$\text{B.C.: } u(t,0) = \frac{\partial u(t,0)}{\partial x} = \frac{\partial^2 u(t,\ell)}{\partial x^2} = \frac{\partial^3 u(t,\ell)}{\partial x^3} = 0, \tag{4}$$

where $u_0(x)$ and $\dot{u}_0(x)$ are known functions.

It is difficult to measure the transverse displacement of the flexible cantilevered beam directly. In this paper, in order to obtain the observation data of the beam, its deformation is measured by N strain sensors located at ξ_j $(0 \leq \xi_j < \ell)$. The observation data of the jth sensor is given by the following manner:

$$y_j(t) = c_j \frac{\partial^2 u(t,\xi_j)}{\partial x^2} + d_j \frac{\partial^3 u(t,\xi_j)}{\partial x^2 \partial t}, \quad (j = 1, \ldots, N), \tag{5}$$

where $\{c_j\}$ and $\{d_j\}$ are known and nonzero constants. In R.H.S. of eq.(5), the first and the second terms represent the beam's strain and its derivative. The second term is required for satisfying the existing condition of the observer mentioned in the next section.

The finite-dimensional model of the beam can be obtained via the modal analysis procedure. The displacement $u(t,x)$ is approximated by a linear combination of mode functions

$$u(t,x) = \sum_{k=1}^{N} u_k(t)\phi_k(x), \tag{6}$$

where $\{u_k(t)\}_{k=1,\cdots,N}$ denote the modal displacements; N is the sufficient number of modes for describing the mechanical behavior of the beam. The associated eigenvalues and mode functions, $\{\lambda_k\}$ and $\{\phi_k(x)\}$, are the solutions of the continuous eigenvalue problem given by

$$\mathcal{A}\phi_k(x) = \lambda_k \phi_k(x), \ (k = 1, \cdots, N), \tag{7}$$

where the operator $\mathcal{A}$ is defined by $\mathcal{A} := (EI/\rho S)d^4/dx^4$ with its boundary conditions

$$\phi_k(0) = \frac{d\phi_k(0)}{dx} = \frac{d^2\phi_k(\ell)}{dx^2} = \frac{d^3\phi_k(\ell)}{dx^3} = 0, \ (k = 1, \cdots, N). \tag{8}$$

The mode functions $\{\phi_k(x)\}$, which are appropriately normalized, can be shown to have orthogonality properties

$$\int_0^\ell \phi_k(x)\, \phi_\nu(x)\, dx = \delta_{k\nu} \tag{9}$$

$$\int_0^\ell \mathcal{A}\phi_k(x)\, \phi_\nu(x)\, dx = \lambda_k \delta_{k\nu}, \tag{10}$$

where $\delta_{k\nu}$ denotes Kronecker delta.

The following set of modal representation model can be obtained from the mathematical model eq.(1), using the orthogonality properties eqs.(9) and (10) as well as the solution in eq.(6):

$$\ddot{u}_k(t) + \frac{c_D}{E}\lambda_k \dot{u}_k(t) + \lambda_k\, u_k(t) = \frac{g}{\rho S} s_k(t; x_c), \quad (k = 1, \cdots, N), \tag{11}$$

where $\{s_k(t;x_c)\}_{k=1,\cdots,N}$ represent the collision inputs in modal representation given by

$$s_k(t;x_c) = \int_0^\ell s(t)\delta(x-x_c)\phi_k(x)dx \tag{12}$$

$$= \phi_k(x_c)\, s(t) \tag{13}$$

which implies that the behavior of $\{s_k(t;x_c)\}$ during the collision depends only on $s(t)$. The position of the collision affects the amplitude of each $s_k(t;x_c)$ as a coefficient.

Let us define a state vector $v(t) := [u_1(t), \cdots, u_N(t), \dot{u}_1(t), \cdots, \dot{u}_N(t)]^{\mathrm{T}}$. We obtain a state space model descried by

$$\dot{v}(t) = Av(t) + B\sigma(t;x_c), \tag{14}$$

where $\sigma(t;x_c) = [s_1(t;x_c), \ldots, s_N(t;x_c)]^{\mathrm{T}}$ which represents the collision input;

$$A = \begin{bmatrix} 0 & I_N \\ -\Lambda_N & -\dfrac{c_D}{E}\Lambda_N \end{bmatrix}, \; B = \begin{bmatrix} 0 \\ \dfrac{g}{\rho S} I_N \end{bmatrix}, \tag{15}$$

and $\Lambda_N = \mathrm{diag}\{\lambda_1, \cdots, \lambda_N\}$; I_* denotes unit matrix.

The observation system can be correspondingly approximated as

$$y(t) = Cv(t), \tag{16}$$

where $y(t) = [y_1(t), \cdots, y_N(t)]^{\mathrm{T}}$;

$$C = [C_c, C_d] \tag{17}$$

$$[C_c]_{ji} = c_j \frac{d^2\phi_i(\xi_j)}{dx^2}, \quad (i = 1, \cdots, N;\; j = 1, \cdots, N) \tag{18}$$

$$[C_d]_{ji} = d_j \frac{d^2\phi_i(\xi_j)}{dx^2}, \quad (i = 1, \cdots, N;\; j = 1, \cdots, N). \tag{19}$$

3. Estimation of Collision Input

The information on the collision spot x_c and its strength $s(t)$ is included in the collision input in modal representation $\{s_k(t;x_c)\}$. However, it is impossible to measure the collision input directly which appears as a disturbance in the mathematical model. In order to obtain the collision input $\{s_k(t;x_c)\}$, it is necessary to base its estimation on the observation data.

Let us examine the procedure for the collision input estimation. Here the relation between the collision input in eq.(14) and the observation data is investigated. Considering the derivative of the observation described by eq.(16), we have

$$\dot{y}(t) = C\,\dot{v}(t). \tag{20}$$

Substituting eq.(14) into eq.(20) and manipulating the resultant equation, $\sigma(t;x_c)$ can be expressed by

$$\sigma(t;x_c) = (CB)^{-1}\{\dot{y}(t) - CAv(t)\}, \tag{21}$$

where the matrix C should hold rank $CB = N$. In R.H.S. of eq.(21), $\dot{y}(t)$ can be obtained using a differentiator. On the other hand, $v(t)$ is the state of the beam which can not be measured. In order to obtain the estimate of the collision input, we consider the following vector $\hat{\sigma}(t)$ via the replacement of the state variable $v(t)$ in eq.(21) by the state estimate $\hat{v}(t)$:

$$\hat{\sigma}(t) = (CB)^{-1}\{\dot{y}(t) - CA\hat{v}(t)\}, \tag{22}$$

where $\hat{v}(t)$ is given by the following full-order observer (Yang and Wilde[12]) for eq.(14), which decouples the effect of the unknown input such as the external force due to the collision. This observer is given by

$$\dot{z}(t) = Fz(t) + Ly(t) \tag{23}$$

$$\hat{v}(t) = z(t) - Ey(t), \tag{24}$$

where $z(t)$ denotes the $2N$-vector; $\hat{v}(t)$ the state estimate of $v(t)$;

$$E = -B(CB)^{-1},\ L = PAB(CB)^{-1},\ P = I_{2N} - EC$$

$$F = T\begin{bmatrix} \tilde{A}_{11} & 0 \\ 0 & \tilde{F}_{22} \end{bmatrix} T^{-1},\ \begin{bmatrix} \tilde{A}_{11} & \tilde{A}_{12} \\ \tilde{A}_{21} & \tilde{A}_{22} \end{bmatrix} = T^{-1}PAT,$$

and T is the matrix which transforms P into its Jordan form. The matrix $\tilde{F}_{22}$ is chosen so that F is stable.

The collision detection problem is to find the time when the collision input $\sigma(t;x_c)$ appears in the R.H.S. of eq.(14). In this paper, the following scalar function $r(t)$, consisting of $\hat{\sigma}(t)$ is used to detect the collision:

$$r(t) := \hat{\sigma}^{\mathrm{T}}(t)\hat{\sigma}(t). \tag{25}$$

To detect the occurrence of collision, we wait the value of $r(t)$ to exceed a preassigned threshold ε.

4. Estimation of Collision Spot

The direct measurement of the collision spot is impossible because of lack of suitable sensors installed on the beam. Fortunately, the relation between the collision spot x_c and the collision input $\{s_k(t;x_c)\}$ was already shown in eq.(13), *i.e.*, the collision input in modal representation consists of the strength of the collision force $s(t)$ and the value of the mode function at the collision spot. The behavior of the collision input depends on $s(t)$ during the collision. On the other hand, the difference between the modes is determined by the value of the mode function at the collision spot, $\{\phi_k(x_c)\}$. Hence, the ratio of the collision inputs corresponding to two different modes can be expressed by a function of collision spot. In this paper we pay attention to the ratio of the collision input corresponding to the first two modes as an indicator to find the collision spot.

Consider a ratio consisting of the collision inputs in the modal representation $s_2(t;x_c)/s_1(t;x_c)$. Substituting eq.(13) into this ratio, it is reduced into a function of x_c, *i.e.*,

$$\frac{s_2(t;x_c)}{s_1(t;x_c)} = \frac{s_0(t)\phi_2(x_c)}{s_0(t)\phi_1(x_c)} = \frac{\phi_2(x_c)}{\phi_1(x_c)} \equiv \theta(x_c),\ \ (t_c \le t \le t_e,\ 0 < x_c \le \ell). \tag{26}$$

This equation implies that the ratio $s_2(t;x_c)/s_1(t;x_c)$ is regarded as a time independent function only during the collision. That is to say, the ratio $s_2(t;x_c)/s_1(t;x_c)$ gives a ratio $\phi_2(x_c)/\phi_1(x_c)$. As a result, we obtain the following relation:

$$\theta(x_c) = \frac{s_2(t;x_c)}{s_1(t;x_c)}, \quad (t_c \le t \le t_e,\ 0 < x_c \le \ell). \tag{27}$$

In this paper, $\theta(x_c)$ is named the mode-function-ratio (MFR).

The problem here is to calculate the collision spot x_c from the MFR. The basic idea to find x_c is as follows. $\theta(x_c)$ is calculated based on the estimate of the collision input. Then inverting $\theta(x_c)$, the collision spot can be obtained from the value of $\theta(x_c)$.

The collision spot x_c can be obtained by inverting the MFR, *i.e.*, $x_c = \varphi(\theta)$, where $\varphi(\cdot)$ denotes the inverse function of the MFR. However, it is difficult to obtain the inverse function of $\theta(x_c)$, analytically, because the MFR is quite complicated function which consists of the mode functions at the collision spot, $\{\phi_k(x_c)\}_{k=1,2}$. Then the MFR can be represented by the Taylor series as follows:

$$\theta(x_c) = \theta(x_0) + \sum_{k=1}^{4} \frac{1}{k!}\theta^{(k)}(x_0)(x_c - x_0)^k + O\left((x_c - x_0)^5\right), \tag{28}$$

where $\theta(x_c)$ is assumed to be monotone and differentiable and x_0 denotes a constant, $0 < x_0 \le \ell$. The series expansion of the inverse of eq.(28) can be expressed by

$$x_c = x_0 + \sum_{k=1}^{4} \alpha_k(\theta - \theta_0)^k + O\left((\theta - \theta_0)^5\right), \tag{29}$$

where $\theta_0 := \theta(x_0)$ and

$$\alpha_1 = b_1^{-1}, \quad \alpha_2 = -\frac{b_2}{b_1^3}, \quad \alpha_3 = -\frac{-2\,b_2^2 + b_3\,b_1}{b_1^5}, \quad \alpha_4 = \frac{-b_4\,b_1^2 + 5\,b_3\,b_2\,b_1 - 5\,b_2^3}{b_1^7}$$

$$b_1 = \left.\frac{d\theta(x_c)}{dx_c}\right|_{x_c=x_0}, \ b_2 = \left.\frac{1}{2}\frac{d^2\theta(x_c)}{dx_c^2}\right|_{x_c=x_0}, \ b_3 = \left.\frac{1}{6}\frac{d^3\theta(x_c)}{dx_c^3}\right|_{x_c=x_0}, \ b_4 = \left.\frac{1}{24}\frac{d^4\theta(x_c)}{dx_c^4}\right|_{x_c=x_0}$$

Although computation of $\theta(x_c)$ requires the true collision input $\{s_k(t;x_c)\}_{k=1,2}$, the available information is the estimate of the collision input in actuality. Then, we consider that $\theta(x_c)$ used in eq.(29) is replaced by the approximation of the MFR which is calculated based on the estimate of the collision input in the time interval $[t, t+\Delta T]$, where ΔT is the short time interval for data collection. Using the least mean square method, the approximation of $\theta(x_c)$ is obtained. Since the relation among $\{s_k(t;x_c)\}_{k=1,2}$ and $\theta(x_c)$ is given by eq.(27), a square error $\{\theta(x_c)\hat{s}_1(t) - \hat{s}_2(t)\}^2$ is considered. Consequently, the approximation of the MFR is regarded as the value of $\hat{\theta}(t)$ so that the following criteria is minimized:

$$J(\hat{\theta}) = \int_{t-\Delta T}^{t} \left\{\hat{\theta}(t)\hat{s}_1(\tau) - \hat{s}_2(\tau)\right\}^2 d\tau. \tag{30}$$

Solving the following equation with respect to $\hat{\theta}(t)$:

$$\frac{\partial J(\hat{\theta})}{\partial \hat{\theta}} = 0, \tag{31}$$

it is given by

$$\hat{\theta}(t) = \frac{h_2(t)}{h_1(t)}, \quad (t_c \le t \le t_e), \tag{32}$$

where

$$h_1(t) = \int_{t-\Delta T}^{t} \hat{s}_1^2(\tau)d\tau, \quad h_2(t) = \int_{t-\Delta T}^{t} \hat{s}_1(\tau)\hat{s}_2(\tau)d\tau.$$

By replacing θ in eq.(29) by $\hat{\theta}(t)$, the estimate of collision spot can be obtained by

$$\hat{x}_c(\hat{\theta}(t)) := x_0 + \sum_{k=1}^{4} \alpha_k \left\{\hat{\theta}(t) - \theta_0\right\}^k, \tag{33}$$

where the high order terms are neglected.

5. Simulation Results

In this section, some numerical results are provided. The beam is assumed to be made of brass with length $\ell = 0.4$ [m], width 4.04×10^{-2} [m], thickness 5.03×10^{-4} [m]. Three strain sensors are patched at $\xi_1 = 4 \times 10^{-2}$ [m], $\xi_2 = 1.6 \times 10^{-1}$ [m] and $\xi_3 = 3.2 \times 10^{-1}$ [m], respectively. The other parameters are set as $c_1 = c_2 = c_3 = 20$, $d_1 = d_2 = d_3 = 10$, $c_D = 4.82 \times 10^8$ [N·s·m^{-2}] and $g = 1$.

The behavior of the flexible beam is generated by solving eq.(11) with respect to the first five modes instead of the partial differential equation described by eq.(1). The initial state of the numerical model is set as $u_1(0) = 1 \times 10^{-6}$, $u_2(0) = 2 \times 10^{-7}$, $u_k(0) = 0$ $(k = 3, 4, 5)$, and $\dot{u}_k(0) = 0$ $(k = 1, \cdots, 5)$. The number of the modeled modes for the observer is set as $N = 3$. We suppose that the collision occurs at $t_c = 3$ [s]. The magnitude of the collision input is generated by the following function:

$$s(t) = 0.1 \sin\left\{\frac{(t-3)\pi}{0.1}\right\}\{u_s(t-3) - u_s(t-3.1)\}, \tag{34}$$

where $u_s(\cdot)$ represents the unit step function. The time division for the numerical model is set as $\Delta t = 1 \times 10^{-3}$ [s].

By solving the eigenvalue problem[13] given by eq.(7) with its boundary conditions eq.(8), the mode function can be obtained as

$$\phi_k(x) = b_k \left[\sqrt{2}\sin\left\{a_k x - \frac{\pi}{4} + (-1)^k \frac{1}{2}\beta_k\right\} - \cos k\pi\, e^{a_k x} \sin\frac{1}{2}\beta_k + e^{-a_k x}\cos\frac{1}{2}\beta_k\right], \tag{35}$$

where $\{b_k\}$ are normalized constants; $a_k = (1/\ell)[(2k-1)\pi/2 - (-1)^k\beta_k]$ and β_k are small positive constants computed by

$$\left.\begin{aligned} \beta_1 &= 0.3043077 \\ \beta_k &= \frac{2}{\alpha} - (-1)^k\frac{4}{\alpha^2} + \frac{34}{3\alpha^3} - (-1)^k\frac{112}{3\alpha^4} + \cdots \end{aligned}\right\} \tag{36}$$

with $\alpha := \exp\{(2k+1)\pi/2\}$. The eigenvalues are $\lambda_k = (EI)/(\rho S)a_k^4$. Concretely, the mode functions with respect to $k = 1$ and 2 can be expressed as follows:

$$\phi_1(x) = -1.02\cos\left(4.70x + 6.33 \times 10^{-1}\right) + 1.09 \times 10^{-1} e^{4.70x} + 0.713\, e^{-4.70x} \tag{37}$$

$$\begin{aligned} \phi_2(x) = &-8.47 \times 10^{-1}\cos\left(11.8x + 7.85 \times 10^{-1}\right) \\ &- 2.32 \times 10^{-4} e^{11.8x} + 5.99 \times 10^{-1} e^{-11.8x}. \end{aligned} \tag{38}$$

Substituting eqs.(37) and (38) with eq.(26) into eq.(28), the MFR for the simulated beam is approximated by the following equation:

$$\theta(x_c) \cong 2.34 - 21.8\ (x_c - 0.2) + 18.5\ (x_c - 0.2)^2 + 113\ (x_c - 0.2)^3 - 22.3\ (x_c - 0.2)^4, \tag{39}$$

where $x_0 = 0.2\,[\mathrm{m}]$; $\theta_0 = 2.34$.

Inverting eq.(39), we obtain the estimate of x_c expressed by

$$\hat{x}_c(\hat{\theta}(t)) = 3.07 \times 10^{-1} - 4.58 \times 10^{-2}\,\hat{\theta}(t) - 1.29 \times 10^{-5}\left(\hat{\theta}(t) - 2.34\right)^2 - 6.33 \times 10^{-4}\left(\hat{\theta}(t) - 2.34\right)^3 + 1.05 \times 10^{-4}\left(\hat{\theta}(t) - 2.34\right)^4. \tag{40}$$

The profile of $\hat{x}_c(\hat{\theta}(t))$ is shown in Fig. 1. The admissible value of the function is in the range between the upper and lower broken line, *i.e.*, $0 \leq \hat{x}_c \leq 0.4$. Furthermore, ΔT in eq.(30) was set as $\Delta T = 0.1$ [s].

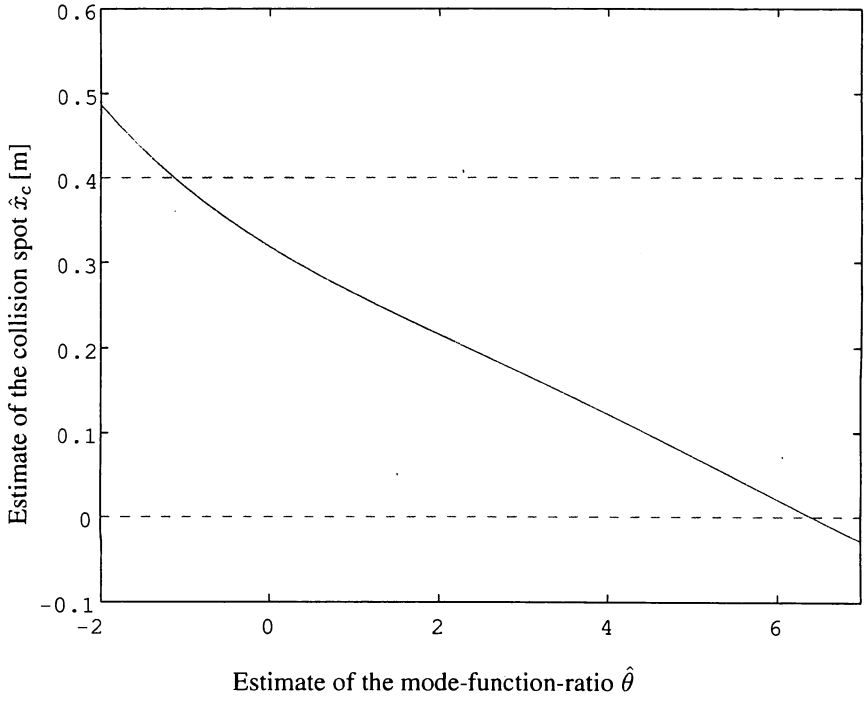

Fig. 1. Profile of $\hat{x}_c(\hat{\theta})$ with respect to $\ell = 0.4\,[\mathrm{m}]$.

The numerical simulations for the eight collision cases were carried out using eq.(40). Figure 2 ($x_c = 0.2\,[\mathrm{m}]$) shows the measurement data obtained using the strain sensors, which clearly shows the collision occurs at $t = 3\,[\mathrm{s}]$. The trajectory of $(\hat{s}_1(t), \hat{s}_2(t))$ is illustrated in Fig. 3. The solid line and the broken line depict the trajectories of the estimate of the collision input $(\hat{s}_1(t), \hat{s}_2(t))$ and the true collision input $(s_1(t; x_c), s_2(t; x_c))$, respectively, where the inclination of the broken line indicates the value of $\theta(x_c)$. Fig. 4. shows the behavior of the collision detection function $r(t)$, where the broken line indicates the threshold value $\varepsilon = 5 \times 10^{-2}$. The estimate of the collision spot $\hat{x}_c(\hat{\theta}(t))$ is shown in Fig. 5. While the value of $r(t)$ exceeds the threshold ε, $\hat{x}_c(\hat{\theta}(t))$ was computed. In theory, the trajectory of $(s_1(t; x_c), s_2(t; x_c))$ draws a straight line (see Fig. 3), because these collision inputs satisfy eq.(27). However, the trajectory of

$(\hat{s}_1(t), \hat{s}_2(t))$ has drawn a slender loop along the true trajectory which is depicted by the broken line. This is due to the estimation error of $\{\hat{s}_k(t)\}_{k=1,2}$. As a result, the estimate of the collision spot x_c shown in Fig. 5 has indicated value, which is larger than true collision spot $x_c = 0.2$ [m].

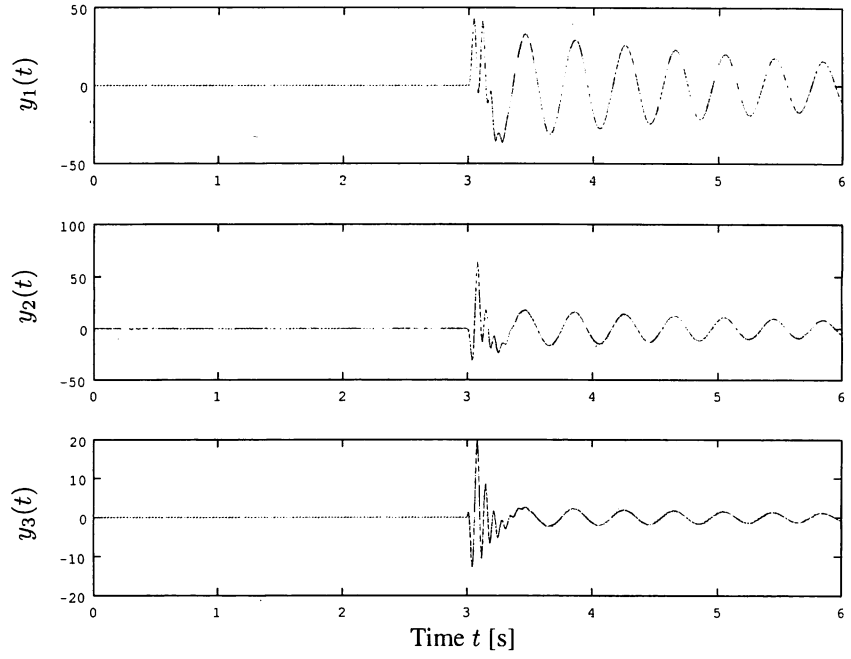

Fig. 2. Observation data, $y_k(t)$ $(k = 1, 2, 3)$, $(x_c = 0.2$ [m]).

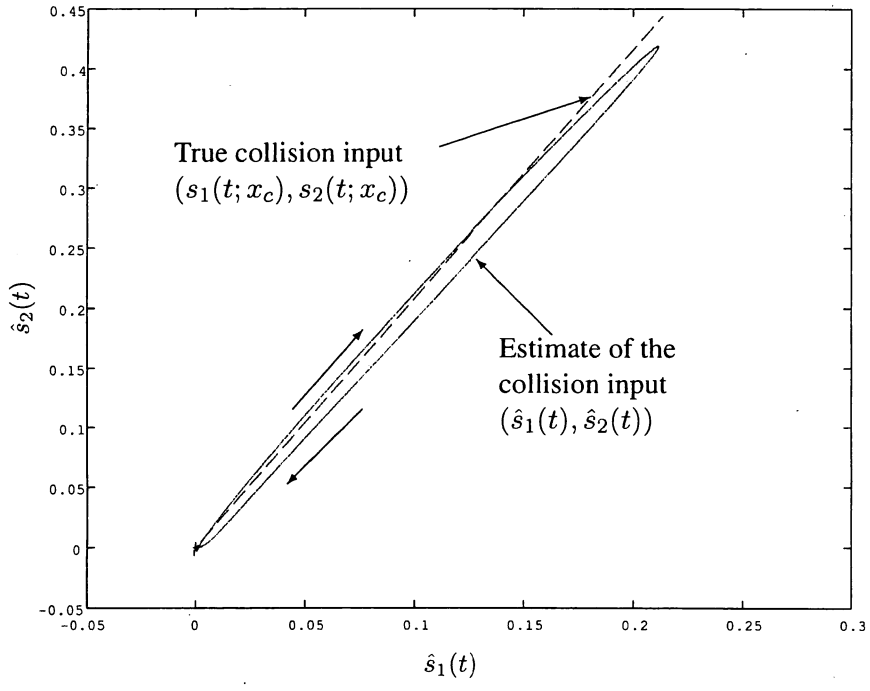

Fig. 3. Trajectory of $(\hat{s}_1(t), \hat{s}_2(t))$, $(x_c = 0.2$ [m]).

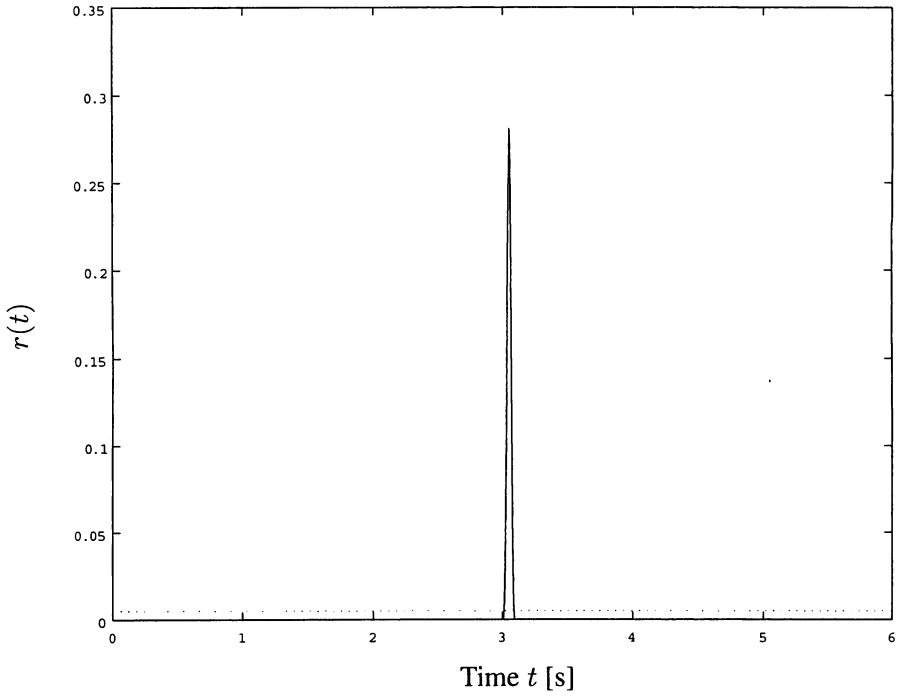

Fig. 4. Behavior of the collision detection function $r(t)$, ($x_c = 0.2$ [m]). The broken line represents the threshold $\varepsilon = 5 \times 10^{-2}$.

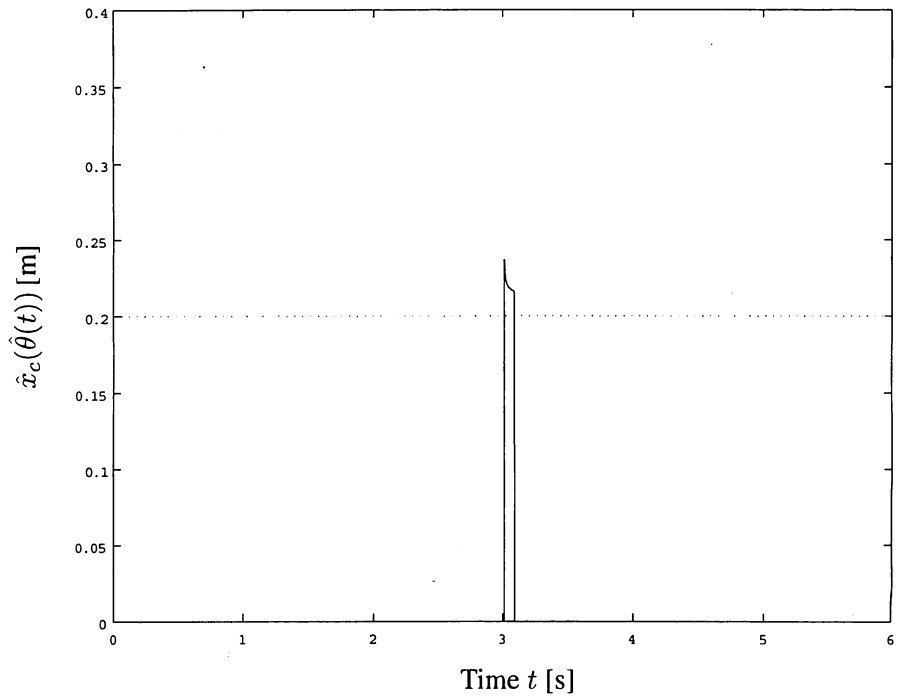

Fig. 5. Estimate of collision spot $\hat{x}_c(\hat{\theta})$, (the broken line depicts the actual collision spot $x_c = 0.2$ [m]).

Table 1. Numerical results of estimation of the collision spots.

Collision spot x_c[m]	Estimate of collision spot $\bar{x}_c$[m]	Error [%]
0.05	0.24	382.52
0.10	0.12	18.35
0.15	0.16	9.44
0.20	0.22	9.84
0.25	0.27	8.69
0.30	0.30	0.11
0.35	0.34	2.52
0.40	0.40	0.53

Table 1 summarizes the simulation results for the eight collision spots and their estimates, where $\bar{x}_c$ denotes the mean value of $\hat{x}_c(\hat{\theta}(t))$ $(t \in D(r(t) > \varepsilon))$ defined by $\bar{x}_c = \int_{D(r(t)>\varepsilon)} \hat{x}_c(\hat{\theta}(t))dt / \int_{D(r(t)>\varepsilon)} 1\, dt$; the error is defined by $100|\bar{x}_c - x_c|/x_c$. This table shows that the collision spot in the range $[0.15, 0.4]$ can be estimated using the proposed method. However, it is difficult to identify the collision spot near the root of the beam, because the estimation error of the collision input is not small in that case. The trajectory shown in Fig. 6 is the simulation result in case the estimation of the collision spot failed (see Table *1*, $x_c = 0.05$ [m]). In this case, since the estimate of the collision input depicts a wide loop, we can not obtain a good estimate of the MFR using the eq.(32).

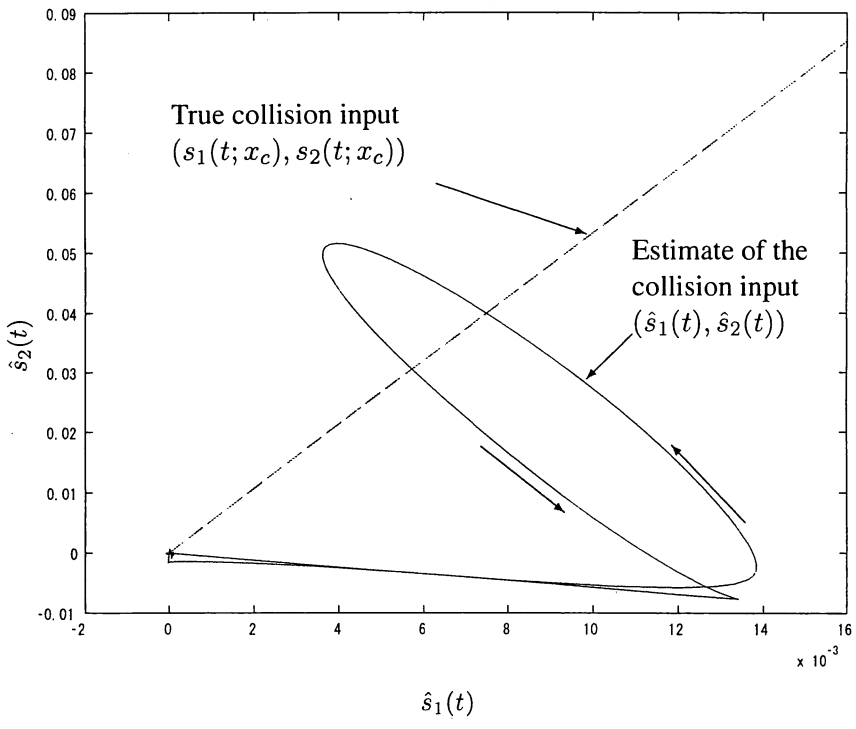

Fig. 6. Trajectory of $(\hat{s}_1(t), \hat{s}_2(t))$, $(x_c = 0.05\,[\mathrm{m}])$.

We can interpret the cause of the estimation error of the collision spot in the following way. The estimation error of x_c depends on the estimation error of $\hat{\theta}(t)$ and the approximation accuracy of $x_c(\theta)$ expressed

in eq.(33). The accuracy of $x_c(\theta)$ is determined by choosing the number of terms. The estimate of the MFR can be expressed using the estimation error of the collision input $\eta(t)$ by

$$\hat{\theta}(t) = \theta(x_c)\frac{\int_{t-\Delta T}^{t} \{s(\tau) + \eta_1(\tau)/\phi_1(x_c)\}\{s(\tau) + \eta_2(\tau)/\phi_2(x_c)\}\, d\tau}{\int_{t-\Delta T}^{t} \{s(\tau) + \eta_1(\tau)/\phi_1(x_c)\}^2\, d\tau}, \tag{41}$$

$$(t_c \le t \le t_e,\ 0 < x_c \le \ell)$$

where $\eta(t) := [\eta_1(t), \cdots, \eta_N(t)]^{\mathrm{T}}$ defined by $\eta(t) = \hat{\sigma}(t) - \sigma(t; x_c)$. Using eq.(21) and eq.(22), the estimation error of the collision input can be described by

$$\eta(t) = (CB)^{-1}CAe(t), \tag{42}$$

where $e(t)$ denotes the estimation error of the observer defined by $e(t) = \hat{v}(t) - v(t)$. When $e(t)$ tends to zero, the estimation error of the collision input $\eta(t)$ given by eq.(42) becomes zero. As a result, $\hat{\theta}(t)$ decribed by eq.(41) approaches to $\theta(x_c)$, when the estimation error of the observer becomes zero.

The large estimation error of the collision spot in the case of $x_c = 0.05$ [m] was caused by the large state estimation error of the observer. If the error of the observer is reduced in the case of collision near the root of the beam, the accuracy of the collision spot estimation will be improved.

6. Conclusion

In this paper an observer-based collision detection and its spot estimation method for a flexible cantilevered beam has been presented. The mathematical model of the beam has been described by the Euler-Bernoulli type partial differential equation. Using the mode expansion method, the mathematical model was reduced into a finite-dimensional model. Introducing the mode-function-ratio and its inverse function given by eqs.(27) and (33), the collision spot estimation based on the observation data has been established. The performance of the proposed method has been demonstrated by numerical simulations.

Acknowledgements

The author wishes to thank Professor Akira Ohsumi, Kyoto Institute of Technology for his useful suggestions and advices. The author would also like to appreciate Mr. Takayuki Sako, Konami Corporation and Mr. Naoto Akiyama, Graduate School of Science and Technology, Kyoto Institute of Technology for making the computer programs. Part of this research was supported by the Ministry of Education, Culture, Sports, Science and Technology of Japan under the Grants-in-Aid for Scientific Research for Encouragement of Young Scientists (B)-14750160.

Department of Mechanical and System Engineering,
Faculty of Enigineering and Design,
Kyoto Institute of Technology,
Matsugasaki, Sakyo-ku, Kyoto 606-8585 JAPAN

References

1) F. Matsuno, T. Asano and Y. Sakawa, *IEEE Trans. Robotics and Automat.*, **10**, pp.287-297 (1994).
2) F. Ching and D. Wang, *Proc. 1999 IEEE Int. Conf. Robotics and Automat.*, pp.419-426 (1999).
3) M. Kaneko, N. Kanayama and T. Tsuji, *Proc. IEEE Int. Conf. Robotics and Automat.*, pp.1113-1119 (1995).
4) M. Kaneko, N. Kanayama and T. Tsuji, *IEEE Trans. Robotics and Automat.*, **14**, pp.278-291 (1998).
5) S. Moorehead and D. Wang, *Proc. IEEE Int. Conf. Robotics and Automat.*, pp.804-809 (1996).
6) Y. Sawada, *Proc. 41st SICE Annual Conf.*, pp.268-273 (2002).
7) Y. Sawada, *Proc. IEEE Int. Conf. Control Applications*, pp.1171-1176 (2002).
8) Y. Sawada, *Proc. 42nd SICE Annual Conf.* pp.2246-2251 (2003).
9) Y. Sawada, *Proc. 34th ISCIE Int. Symp. Stochastic Systems Theory and Its Application*, pp.183-188 (2002).
10) Y. Sawada, *Trans. ISCIE*, **17**, pp.349-357 (2004)(in Japanese).
11) Y. Sawada and T. Sako, *Proc. 35th ISCIE Int. Symp. Stochastic System Theory and Its Applications*, pp.106-111 (2003).
12) F. Yang and W. Wilde, *IEEE Trans. Automat. Contr.*, **33**, pp.677-681 (1988).
13) A. Ohsumi and Y. Sawada, *Trans. ASME, J. Dynamic Systems, Measurements, and Control*, **115**, pp.649-657 (1993).